PURD-TH-99-08, astro-ph/9911218

Short-scale gravitational instability in a disordered Bose gas

S. Khlebnikov
Department of Physics, Purdue University, West Lafayette, IN 47907, USA
(November 1999)

Abstract

We study numerically evolution of a self-gravitating nonequilibrium Bose gas contained in a fixed volume. We find that, even when the volume is small enough to prevent collisionless instability, a compact phase-correlated object (a Bose star) can form, by gravity alone, from a disordered initial state. We interpret this effect and the associated growth of the density contrast as consequences of a new type of gravitational instability—a nonlinear instability due to stimulated gravitational scattering of the bosons. Our results imply that formation of Bose stars, in regions that have fallen out of the Hubble expansion, may be a quite general phenomenon, not requiring a large preexisting correlation length or any short-range interactions.

I. INTRODUCTION

Gravitational (Jeans [1]) instability is believed to be at the root of all the large-scale structure that we observe in the universe. (For a review on structure formation, see ref. [2].) The instability is a direct consequence of gravity being an attractive force: particles will accrue on small clumps, and the clumps will get bigger. Jeans's original calculation was based on description of matter via classical hydrodynamics. This description applies only at spatial scales larger than the mean-free path of the particles (which is defined here with respect to some interaction other than gravity). Evolution of density perturbations with scales smaller than the mean-free path can for many purposes be described by the collisionless Vlasov approximation—unless the scale is so small that this semiclassical method breaks down. In the collisionless approximation, a self-gravitating gas is unstable with respect to sufficiently long-wave perturbations, and the instability is of the same type as Jeans's. (We will define later more precisely what "the same type" means.)

For a wide class of initial distributions, however, the collisionless instability disappears for short-scale perturbations. Consider, for example, a homogeneous (on average) nonrelativistic gas of particles of mass m in a box of fixed size, in the Newtonian approximation to gravity (in addition, we assume that the uniform component of density does not gravitate). We show in Appendix that, for the class of momentum distributions defined there, the collisionless instability exists only for density perturbations with wavenumbers

$$k < Ck_J^2/k_0 \equiv k_* \ , \tag{1}$$

where k_0 is a typical momentum of the particles, and C is a numerical constant depending on their momentum distribution. (We use a system of units with $\hbar = 1$.) The wavenumber k_J is determined by the average density number $n_{\rm ave}$:

$$k_J^4 = 16\pi G m^3 n_{\rm ave} \ , \tag{2}$$

and will be called the Jeans wavenumber. One may wonder if any gravitational instability exists for perturbations with $k > k_*$, that is at shorter scales.

The condition (1) suggests that, depending on the relation between k_0 and k_J, a self-gravitating gas can be in one of two different regimes. When

$$k_J \gg k_0 \ , \tag{3}$$

eq. (1) shows that collisionless instability occurs for perturbations with all wavenumbers up to $k \sim k_0$, at which point the semiclassical description of particles breaks down, and the Vlasov equation can no longer be used. In at least one case, however, one can show that a linear instability exists even for $k > k_0$ (although of course the argument cannot be based on the Vlasov equation). This case is a perfectly ordered Bose gas, i.e. a gas in which all particles are Bose-Einstein condensed in the $k = 0$ mode. Elementary excitations of this Bose-Einstein condensate are Bogoliubov's quasiparticles, and their dispersion law is known, from Bogoliubov's work [3], for arbitrary two-body potential. When the only interaction between particles is Newtonian gravity, the dispersion law (for a nonrelativistic gas) reads

$$\omega(k) = (1/2m)\left[k^4 - k_J^4\right]^{1/2} \ , \tag{4}$$

which means that the perfectly ordered Bose gas is gravitationally unstable for all $k < k_J$. This result had been reported previously in a number of papers [4,5]. (We have presented it here for a region that is out of the Hubble expansion; a treatment in the expanding universe is also available [5,6].)

The perfectly ordered state is just one possible initial state of a Bose gas. A generic initial state is a patchwork of correlated domains, rather than one such domain. If we describe a nonrelativistic Bose gas by a complex field ψ, correlated regions are those in which the phase of ψ is more or less constant in space. The typical size of correlated regions is $2\pi/k_0$. If such a region contains many particles, we can apply formula (4) to it individually, but only for wavenumbers $k \gg k_0$: only these sample a more or less ordered background. Eq. (4) then predicts an instability for k in the range $k_0 \ll k < k_J$. At $k \sim k_0$, we expect this instability to cross over smoothly to the instability found in the Vlasov approximation. Thus, we expect that a nonrelativistic Bose gas satisfying the condition (3) is unstable with respect to density perturbations with all wavenumbers $k < k_J$ (although the theoretical description of the instability has to be switched at $k \sim k_0$).

We can now formulate more precisely what we mean by saying that the gravitational instability in the perfectly ordered Bose gas is of the same type as the instability found by Jeans for matter described by classical hydrodynamics. The similarity has two closely related aspects. First, in either case, the instability is *linear*, i.e. density perturbations with different wavenumbers do not have to interact with one another for it to occur. Second, the growth rate of the instability, for low-k modes, scales as square root of the average number density:

$$\mathrm{Im}\omega(0) \propto \sqrt{n_{\mathrm{ave}}} \tag{5}$$

(see e.g. eq. (4)). One can say that this square-root scaling law defines a certain "universality class", to which the original Jeans instability, the collisionless instability, and the instability of the ordered Bose gas all belong.

In this paper, we want to consider a nonrelativistic Bose gas in which the relation between k_0 and k_J is reversed compared to (3):

$$k_J \ll k_0 \ . \tag{6}$$

Our motivation is simply that we do not know at present which type of initial state is more likely to be realized in the early universe. We will call the case (6) *disordered* (because correlated domains are initially small), as opposed to the case (3), which we will call *ordered* (initial correlated domains are large). According to eq. (1), the collisionless instability will occur in a disordered gas only at large spatial scales. So, if there is a gravitational instability on shorter scales, it is caused by gravitational scattering of the particles, rather than by collisionless effects. Our goal was to determine effects of gravitational scattering on the evolution of a disordered Bose gas.

We imagine the following sequence of events in the early universe. A disordered Bose gas first becomes unstable with respect to large-scale density perturbations via the collisionless (Vlasov) mechanism. As clumps formed by this mechanism grow denser, collisionless instability can develop on shorter scales. We expect that this process will give rise to clusters of

matter, each cluster including a number of smaller clumps and some inter-clump gas. Gravitational scattering, which is a slower process, will operate inside those clusters, after they have already fallen out of the Hubble expansion. Accordingly, we considered a disordered Bose gas in a box of fixed size. In addition, we used Newtonian gravity, which we expect to be good for sufficiently short-scale perturbations.

Our results, obtained by numerically following the evolution of a random classical field, apply when the initial state has large (compared to unity) occupation numbers at low momenta and little occupation at high momenta. These results are as follows. (i) Starting from a disordered state, we have observed a well-defined crossover from collisionless instability to a slower growth of the density contrast. This slower growth can be viewed as a gravitational instability of a different type than the linear instabilities discussed above. We confirm the existence of this new type of gravitational instability by running simulations in smaller boxes, so as to remove the collisionless instability altogether. In this case, any growth of the density contrast will have to be attributed to some new type of instability. We indeed observe such a growth, and we interpret it as a result of gravitational scattering of the bosons. The scaling of the rate of the growth with $n_{\rm ave}$, in a small box, is quite distinct from the square-root law (5). In this sense, the new instability is in a different "universality class" than the linear instabilities. (ii) Clumps that result from this nonlinear instability are phase-coherent; in other words, the instability leads to formation of Bose stars. (By a Bose star we mean any coherent gravitationally bound configuration of a Bose field; ground states of gravitating bosons were originally discussed in ref. [7].) It has been long considered possible that Bose stars will form as result of the linear instability in an ordered Bose gas [5,8] (although, to our knowledge, that had not been actually demonstrated). Formation of Bose stars in an initially disordered gas is a different effect. We attribute it to gravitational scattering in our case being *stimulated*: as an effect of Bose statistics, particles that scatter into regions of high density will prefer to end up in phase with particles that are already there.

The rest of the paper is organized as follows. Sect. 2 contains formulation of the problem in terms of a random classical field. In Sect. 3 we present numerical results. Our conclusions, and connections to earlier work, are given in Sect. 4. Some technical details concerning the collisionless instability are given in Appendix.

II. SETTING UP A RANDOM CLASSICAL FIELD

We consider a nonrelativistic Bose gas described by the following equations:

$$i\frac{\partial\psi}{\partial t} = -\frac{\nabla^2}{2m}\psi + m\Phi\psi + g_4\psi^\dagger\psi^2 \; ; \tag{7}$$

$$\nabla^2\Phi = 4\pi G m(\psi^\dagger\psi - n_{\rm ave}) \; . \tag{8}$$

Here ψ is a complex Bose field, and Φ is the (real) gravitational potential. Number density of bosons is $n = \psi^\dagger\psi$, and its volume average is called $n_{\rm ave}$. For reasons given in the introduction, we assume it sufficient to consider the gas in a box of fixed size (rather than in an expanding universe) and to use the Newtonian approximation to gravity.

All numerical results presented in the next section are for $g_4 = 0$, i.e. for the case when gravity is the only interaction between the particles. The method that we use can be applied

equally well to the case $g_4 \neq 0$. In this paper, however, we limit ourselves to only a cursory discussion (in the concluding section) of possible effects of short-range interactions.

The field ψ is in principle a quantum operator but here we treat it as a random classical field. Usefulness of this classical approximation has been recently emphasized in connection with a number of problems in nonequilibrium statistics of Bose fields. Among these problems, the one closest to the problem at hand is phase separation in a nonequilibrium Bose gas with a *local* attractive interaction (and a repulsive interaction at larger densities) [9]. Some of the results that we obtain here, notably, the coherent nature of the clumps, are similar to those for a local interaction, but due to the long-range nature of gravity there are also some differences. For example, for a short-range interaction, one can also identify ordered and disordered types of initial states. Results of ref. [9] correspond to a disordered initial state. For neither type of state, however, we expect a large-distance crossover to collisionless (Vlasov) dynamics.

The system (7)–(8) can be viewed as a modification, required to include Newtonian gravity, of the Gross-Pitaevskii (GP) equation familiar from the theory of laboratory Bose gases [10]. The system (7)–(8) is universal in the same sense as the GP equation is: at low gas densities, the only parameter needed to characterize short-range interactions is the scattering length, which is encoded in the coupling constant g_4.

The classical approximation is good when the field ψ is large and its power spectrum is contained at small momenta: speaking in terms of particles, the occupation numbers in low-momentum modes are much larger than unity, while those in high-momentum modes are small and rapidly decrease with momentum. We stress, however, that when scattering is strong, as it may become at later stages of clumping, the very notion of a particle, as an entity propagating for relatively large times without collisions, becomes ill-defined. One of the useful features of the classical approximation is that it allows one to avoid dealing with that notion altogether. In addition, provided the power spectrum of ψ satisfies the necessary conditions, the classical approximation will apply equally well either in the ordered or in the disordered case. We also stress that, although this may sound paradoxical, the classical approximation does take into account effects of the quantum Bose statistics of the particles. Indeed, the very possibility for ψ to become (almost) classical, in the limit of large occupation numbers, is one such effect.

For numerical simulations presented in this paper, we have chosen the initial power spectrum of ψ in the following simple form (cf. ref. [9]):

$$|\psi_{\mathbf{k}}|^2 = A \exp(-k^2/k_0^2) \ , \tag{9}$$

where $\psi_{\mathbf{k}}$ are Fourier components of the field ψ:

$$\psi(\mathbf{r}) = V^{-1/2} \sum_{\mathbf{k}} \psi_{\mathbf{k}} \exp(i\mathbf{kr}) \ , \tag{10}$$

V is the integration volume. For an ideal gas, $|\psi_{\mathbf{k}}|^2$ would be the conventionally defined occupation numbers; we will often use the same terminology for the interacting gas. For the classical approximation to apply, it is sufficient that $A \gg 1$. Although the distribution (9) may look like an equilibrium Maxwell distribution, it is totally unrelated to the latter. The Maxwell distribution follows from the Bose distribution in the limit when the occupation numbers are small. In our case, $A \gg 1$, and the occupation numbers (at low wavenumbers)

are large. Thus, the spectrum (9) is highly nonthermal. Eq. (9) determines the magnitudes of $\psi_{\mathbf{k}}$. The phases of $\psi_{\mathbf{k}}$ are chosen as uncorrelated random numbers. The initial number density contrast corresponding to these initial conditions is $\delta n/n \approx 1$.

Bose gases with highly nonthermal spectra can form in the early universe through various nonequilibrium processes, such as spinodal decomposition or postinflationary reheating. (Formation of nonthermal spectra in the latter case is reviewed in [11].) We do not pretend that the specific form (9) is in any way realistic. We only use it as a representative of spectra satisfying the conditions of applicability of the classical approximation. We have also considered some different forms of the initial spectra and have convinced ourselves that these modifications do not alter the results in any significant way.

Finally, for comparison with the classical method used here, we review results obtained in the collisionless (Vlasov) approximation. Evolution of density perturbations with wavenumbers $k \ll k_0$ can be studied by considering particles as semiclassical wave packets. We stress that this semiclassical approximation for the particles is entirely different from the classical approximation for the field ψ. In particular, it does not require that the occupation numbers be large but requires that perturbations be slowly varying. (It is the other way around for the approach based on a random classical field.) When the semiclassical view of the particles applies (i.e. a perturbation is slowly varying), one can describe them with a classical distribution function $f(\mathbf{r}, \mathbf{p}; t)$, which is proportional to the Fourier transform, with respect to $\mathbf{k}$, of the quantum average of $\psi^\dagger_{\mathbf{p}-\mathbf{k}/2}\psi_{\mathbf{p}+\mathbf{k}/2}$. The distribution function, together with the gravitational potential Φ, can be used to construct a collisionless approximation (which, if needed, can be augmented by a collision integral). The construction is entirely analogous to the derivation of the Vlasov equation for plasmas, see e.g. [12]. In the collisionless approximation, we find that frequencies $\omega(\mathbf{k})$ of small perturbations of a homogeneous state with a distribution function $f_0(\mathbf{p})$ are determined by the dispersion equation

$$1 + \frac{4\pi G m^2}{k^2} \int \mathbf{k} \frac{\partial f_0}{\partial \mathbf{p}} \frac{d^3p}{\mathbf{kv} - \omega - i0} = 0 \,, \tag{11}$$

where $\mathbf{v} = \mathbf{p}/m$. When kv, for a typical v, is much smaller than $|\omega|$, the dispersion equation reduces to

$$1 + 4\pi G m n_{\rm ave}/\omega^2 = 0 \,. \tag{12}$$

Eq. (12) shows that there is a linear instability with the growth rate

$$\omega_i(0) = (4\pi G m n_{\rm ave})^{1/2} = k_J^2/2m \,. \tag{13}$$

For a wide class of initial distribution functions, which is specified in Appendix, the collisionless instability disappears at $k \geq k_*$, where k_* is estimated as in the condition (1). The precise value for k_* is obtained by setting $\omega = 0$ in eq. (11) and solving for k. (This procedure is justified in the Appendix.) For example, in an initial state with power spectrum (9) the distribution function is

$$f_0(\mathbf{p}) = \frac{A}{(2\pi)^3} \exp(-p^2/p_0^2) \,, \tag{14}$$

where $p_0 = k_0$ in the system of units with $\hbar = 1$. In this case, collisionless instability occurs only for

$$k < k_* = (\xi/2)^{1/2} k_0 \ , \tag{15}$$

where $\xi = k_J^4/k_0^4$. Eq. (15) is equivalent to (1) with $C = 1/\sqrt{2}$.

III. NUMERICAL RESULTS

For numerical work, it is convenient to rescale the fields of our model, so that we have to deal with a smaller number of parameters. Define new fields χ and ϕ as

$$\chi = (8\pi G m^3)^{1/2} \psi \ , \tag{16}$$

$$\phi = 2m^2 \Phi \ . \tag{17}$$

Then, eqs. (7)–(8) with $g_4 = 0$ take the form

$$2mi \frac{\partial \chi}{\partial t} = -\nabla^2 \chi + \phi \chi \ , \tag{18}$$

$$\nabla^2 \phi = \chi^\dagger \chi - \nu_{\rm ave} \ , \tag{19}$$

where $\nu_{\rm ave}$ is the average of $\nu = \chi^\dagger \chi$ over space. Initial condition (9) takes the form

$$|\chi_{\mathbf{k}}|^2 = B \exp(-k^2/k_0^2) \ , \tag{20}$$

where $B = 8\pi G m^3 A$, and $\chi_{\mathbf{k}}$ are related to $\chi(\mathbf{r})$ in the same way as $\psi_{\mathbf{k}}$ to $\psi(\mathbf{r})$, see eq. (10). Finally, the expression (2) for the Jeans wavenumber reduces to

$$k_J^4 = 2\nu_{\rm ave} \ . \tag{21}$$

All data presented in the figures were obtained by numerically integrating the system (16)–(17), with initial power spectra of the form (20) and uncorrelated random initial phases for $\chi_{\mathbf{k}}$, on 64^3 cubic lattices with periodic boundary conditions. We have chosen the unit of length so that $k_0 = 2\pi$, and the unit of time so that $2m = 1$. The integrations were done using a second-order in time operator-splitting algorithm; updates corresponding to the operator ∇^2 were carried out by a spectral method based on the fast Fourier transform. The algorithm conserves the number of particles exactly; energy nonconservation was below 1% for all the data sets represented in the figures.

As we have mentioned in the introduction, there are basically two choices for the size of the integration box. One possibility is to choose the box large enough to activate collisionless instability, in order to see a crossover from the collisionless instability to a different regime. While it is clear, even a priori, that a linear instability cannot carry on forever and will have to end somehow, it is still interesting to see explicitly how that happens and what the different regime is. Representative results are shown in Fig. 1. These results are for $B = 20$ and box size $L = 4.25$. A crossover, around $t = 1.2$, from a more rapid to a slower overall growth is seen both in the density contrast and, especially, in the ratio of the total potential and kinetic energies. The density contrast is defined as

$$\delta n/n = \langle (\nu - \nu_{\rm ave})^2 \rangle^{1/2} / \nu_{\rm ave} \ , \tag{22}$$

where the brackets denote averaging over space. It is significant that the growth of the density contrast continues after the linear instability apparently terminates. This allows us to speak about a *nonlinear instability*, which we attribute to gravitational scattering. The overall growth of the density contrast is superimposed on rapid oscillations, which are especially large at the later, scattering stage. We attribute these oscillations in the density contrast to oscillations of matter about a forming star.

To confirm the existence of a nonlinear instability, it is useful to run simulations in a smaller box, so that the long-wave modes that could undergo the collisionless (linear) instability are eliminated. For a cubic box with periodic boundary conditions, this means choosing the side length L so that $2\pi/L$ is larger than the wavenumber k_* that appears on the right-hand side of (1) (there are no density perturbations with $k = 0$ because the total number of particles is conserved). Any growth of the density contrast in an initially disordered gas in such a box will have to be attributed to some new type of gravitational instability. We can find out if this instability belongs to a new "universality class" by studying how its rate depends on the initial density of the gas.

When gravity is the only interaction between the particles, the rate of clumping, during an initial stage when the gas is still nearly uniform, can be written in general as

$$t_c^{-1} = \frac{k_0^2}{2m} F(k_J^4/k_0^4, k_* L) \; . \tag{23}$$

The function F depends on two parameters that measure the strength of gravitational interaction between the particles:

$$\xi = k_J^4/k_0^4 \tag{24}$$

measures the strength of interactions for momentum transfers of order $2\pi/k_0$, while $k_* L$ measures that for momentum transfers of order $k_{\min} = 2\pi/L$. In the limit $k_* L \to \infty$, when the initial clumping is due to collisionless instability, F becomes a function of its first argument only, and

$$F(\xi) \propto \sqrt{\xi} \; , \tag{25}$$

see (12). In an ordered Bose gas, dependence of the rate on L disappears whenever $k_J \gg k_{\min}$, and it scaling with ξ is then given by the same square-root law (25), see (4).

In an initially disordered gas, situation is more complicated. The condition (6) (i.e. $\xi \ll 1$) guarantees only that interactions in the initial state are weak for momentum transfers of order $2\pi/k_0$. In a small box, we also have the condition $k_* < k_{\min}$, which guarantees that interactions are at most of moderate strength even for the smallest momentum transfers. In this case, the initial gas can be considered weakly interacting, and one may contemplate applying kinetic theory. However, even if suitable kinetic equations exist, they will, in general, not reduce to a Boltzmann equation (properly modified to include the effect of large occupation numbers). Indeed, as we have already noted, fluctuations with spatial scales $\ell \lesssim 2\pi/k_0$ cannot be described using the conventional semiclassical distribution function. If such fluctuations are important (and we will argue that in the present case they are), the Boltzmann equation will not apply.

The simplest way to see that the Boltzmann equation is in general insufficient for studying evolution of a Bose gas, either for long-range or for short-range interactions, is to note that it

includes interaction only via the scattering probability and so does not distinguish between attractive and repulsive interactions. On the other hand, on physical grounds we expect dynamics for these two types of interactions to be vastly different.

Let us refer to the rate predicted by the Boltzmann equation for changes in the distribution function as the Boltzmann rate. For a short-range attractive interaction, it has been found numerically in ref. [9] that scaling of the clumping rate with ξ agrees to a good accuracy with scaling of the Boltzmann rate. In general, however, there is no reason to expect such agreement. For gravitational scattering, the Boltzmann rate (for a gas with large occupation numbers) is of the form (23) with

$$F(\xi, k_* L) \propto \xi^2 \ln(k_0 L) \; . \tag{26}$$

The logarithm here is analogous to the Coulomb logarithm in plasma kinetics (cf. ref. [12]); it is due to an infrared divergence in the collision integral. In a small box, this divergence is cut off at wavenumber transfers of order $k_{\min} = 2\pi/L$. Now, consider the case when k_0 and L are fixed. The scaling predicted by (26) is $F(\xi) \propto \xi^2$. This is not quite what we see numerically. Instead, a good fit to the rate is obtained with

$$F(\xi) \propto \xi^\alpha \; . \tag{27}$$

where α is noticeably larger than 2.

We attribute this large deviation of α from 2 to an important role played by fluctuations with spatial scales much smaller than $2\pi/k_0$. One can readily invent a reason why such fluctuations are more important in the presence of a long-range interactions than in the absence of such: even a short-scale fluctuation will influence many particles when there is a long-range force. We thus arrive at a picture of short-scale fluctuations constantly appearing and disappearing, until one of them is able to start a growing clump.

To extract the scaling law from our numerical results, we have used data corresponding to $L = 3.5$ and three different values of B: $B = 7$, $B = 10$ and $B = 20$. The corresponding values of $\xi = k_J^4/k_0^4$ are 0.050, 0.071, and 0.143. For these values of L and ξ , the right-hand side of (15) is smaller than $2\pi/L$, so collisionless instability does not occur. Consequently, the density contrast's growth, which was observed in all three cases, is a signature of a new type of gravitational instability.

The growth of the density contrast should be more accurately referred to as a growth of some average with respect to time, because it is superimposed on rapid oscillations similar to those seen at later stages in Fig. 1. We expect that such an average will depend on time and ξ mainly through a dependence on the ratio t/t_c, or, because k_0 and L are kept constant, through the product $t\xi^\alpha$, where α is the power that we want to determine:

$$\overline{\delta n/n} \approx f(t\xi^\alpha) \; . \tag{28}$$

The overline denotes averaging over several oscillations, and f is some function. When we plot the averaged density contrast, for the above three values of B, against the rescaled time variable $t\xi^\alpha$, we find that a good collapse of the plots is achieved for

$$\alpha = 2.7 \; , \tag{29}$$

see Fig. 2. The collapse is not nearly as good for $\alpha = 2$, the value characteristic of a Boltzmann rate. Our interpretation is that the instability is a result of gravitational scattering, in which fluctuations with spatial scales $\ell \ll 2\pi/k_0$ play an important role.

There is an approximately linear stage in the growth of $\overline{\delta n/n}$ in Fig. 2, from about 0.5 to about 1.2 in units of $100t\xi^{2.7}$. Fitting this linear growth with a time dependence of the form

$$\overline{\delta n/n} = t/t_c + \text{const} \ , \tag{30}$$

provides one possible definition of the rate t_c^{-1}. Numerical fitting gives

$$t_c^{-1} \approx 250\xi^{2.7} \ . \tag{31}$$

This corresponds to eq. (23) with $F(\xi) \approx 6\xi^{2.7}$.

The estimate (31) has been obtained for initial power spectra of the form (9). It is natural to expect that a different form of the initial power spectrum will lead to a different numerical coefficient in (31). That is indeed so, although in cases that we have considered the difference is not overwhelming. For instance, one can generate a random field with a power spectrum of the form (9) and then make, by hand, the magnitudes of χ on all lattice sites equal to some fixed value, while preserving the phases (in coordinate space). One can then use this new field as an initial condition that has a power spectrum different from (9). We have done that for $L = 3.5$, and $B = 10$ and 20. In this case, the density contrast is initially zero. However, it rapidly develops to a nonzero value, as dynamics of the density is activated by dynamics of the phase of ψ. The subsequent evolution of the density contrast is fairly similar to that seen in Fig. 2. The scaling of the rate is consistent with $\alpha = 2.7$, but the rate itself is about half of that given by eq. (31).

Finally, Fig. 3 shows the profile of the star at different moments of time, and Fig. 4 illustrates the star's phase-correlated (Bose-Einstein condensed) nature. (Only one large star has formed per box, in addition to a number of much smaller clumps.)

IV. DISCUSSION

The main result of this work is numerical evidence for a new type of gravitational instability. We have observed this instability in simulations of a disordered Bose gas in a box of a fixed size. We interpret it as being due to collisions between the particles, or, in terminology more suitable for a system with large occupation numbers, between classical waves. We have found that scaling of the instability rate with the average density deviates from the behavior characteristic of changes described the Boltzmann equation. We interpret this deviation as an indicator of an important role played by short-scale fluctuations of the field. We have also presented evidence (Fig. 1) that this instability will take over from a collisionless instability in a large system. This means that it could contribute to formation of structures inside regions that had already fallen out of the Hubble expansion. In addition, we have found that this collisional instability leads to formation of a phase-correlated clump of matter (a Bose star) in an initially disordered Bose gas. Hence, Bose stars can form through gravity alone even in the absence of a large preexisting correlation length.

These results were obtained using the classical approximation for a Bose field. The classical approximation applies to a field that has a certain type of nonthermal power spectrum, namely, occupation numbers are large at small wavenumbers but rapidly decrease towards the ultraviolet. We do not exclude, however, that a similar nonlinear instability exists in matter with different distributions of particles with respect to momenta, for example, in a thermal or nearly thermal gas (for which the classical approximation does not apply).

Our results may apply to nonbaryonic dark matter (if the dark-matter particle is a boson) and to low-density hydrogen. (At high densities, when inelastic processes are important, the simple description (7) is no longer adequate.) It is fascinating to think that some of the matter in the universe may be in the form of superfluid hydrogen. However, there may be interesting implications for structure formation even if our results apply only during initial stages of clumping, when the density is still low.

We should also comment on a possible role of short-range interactions in a disordered self-gravitating Bose gas. As we have already mentioned, at low enough densities all the short-range interactions will be encoded in a single coefficient g_4 of the cubic term in eq. (7). The strength of this local interaction relative to the strength of gravitational scattering in the initial state is measured by the parameter $\eta = g_4 k_0^2/4\pi G m^2$. This parameter can be small even when g_4 is much larger than G/c^2 (c is the speed of light), provided the ratio k_0/mc is small enough, i.e. the initial state is sufficiently nonrelativistic. On the other hand, a not-too-small η can lead to interesting effects. A repulsive interaction ($g_4 > 0$) in a Bose gas causes coarsening—growth of the sizes of correlated domains [13]. If the interaction is strong enough, we expect that the gas will become sufficiently ordered before the nonlinear instability had a chance to develop, and clumping will take place via the corresponding linear instability. In addition, we expect that repulsion will make emerging Bose stars larger in size and smaller in density. (For equilibrium configurations, it has been long known that even a small repulsion makes a large difference [14].) An attractive interaction ($g_4 < 0$) produces correlated clumps all by itself [9]; we expect that it will help gravity along when both are present.

Finally, we discuss relation of our work to earlier work in the literature. We can discern two trends in the earlier work on formation of Bose stars. Some researchers considered gravitational stability and evolution of already coherent configurations. That work included linear stability analysis of a homogeneous Bose-Einstein condensate [4,5] and a study of spherically symmetric collapse of an already coherent spherically symmetric configuration [15]. It has been suggested [5,8] that the Jeans-type instability of a homogeneous Bose-Einstein condensate may lead to formation of Bose stars. Although we do not present corresponding data in this paper, we have confirmed that a Bose star indeed forms in an ordered Bose gas. However, we have given evidence that a large preexisting correlation length, i.e. a high initial degree of spatial coherence, is not necessary for Bose star formation. A Bose star can form even in an initially incoherent (disordered) gas via a new type of gravitational instability that we have identified here. The second trend in the earlier work was to consider ordering effects of local interactions. In particular, it has been argued that due to effects of the Bose statistics even a very weak interaction, such as that between axions, can result in a relaxation time comparable to the age of the universe [16], and, as a consequence, a Bose star may form out of an initially incoherent clump [17]. Here we have shown that phase coherence can develop due to gravity alone, in the absence of any

additional interaction.

The author thanks F. Finelli and I. Tkachev for discussions. This work was supported in part by the U.S. Department of Energy under Grant DE-FG02-91ER40681 (Task B).

APPENDIX: MORE ON THE COLLISIONLESS INSTABILITY

In this appendix we will show that for a wide class of initial distribution functions the collisionless instability (such as found in the Vlasov approximation) disappears at sufficiently large wavenumbers. Whether the instability is present or absent is determined from the dispersion relation (11), which we rewrite here as

$$\gamma(\omega, k) = 0 \ , \tag{A1}$$

where γ is the "gravitational permittivity":

$$\gamma(\omega, k) = 1 + \frac{4\pi G m^3}{k^2} \int_{-\infty}^{\infty} dp_x \frac{g'(p_x)}{p_x - m\omega/k - i0} \ . \tag{A2}$$

We have oriented coordinate axes so that $\mathbf{k} = (k, 0, 0)$, with $k > 0$, and defined a distribution function with respect to p_x:

$$g(p_x) = \int dp_y dp_z f_0(p_x, p_y, p_z) \ . \tag{A3}$$

In an isotropic medium, the form of $g(p_x)$ would not depend on the direction of x (that is the direction of $\mathbf{k}$), but we do not assume isotropy here.

By its physical meaning, $g(p_x)$ is nonnegative. We assume that for any direction of $\mathbf{k}$ the function $g(p_x)$ satisfies the following conditions: (i) $g(p_x)$ is smooth (infinitely differentiable) and decreases with $|p_x|$ rapidly enough for the integral in (A2) to be convergent for any ω with $\mathrm{Im}\omega > 0$. (ii) $g(p_x)$ is even; (iii) $g(p_x)$ is monotonically decreasing for all $p_x > 0$. From these conditions, two more follow: (iv) $g'(0) = 0$; and (v) $g''(0) < 0$. Primes denote derivatives with respect to p_x.

Eq. (A2) defines an analytic function in the upper half-plane of complex ω; in our definition, the upper half-plane does not include the real axis. To obtain $\gamma(\omega, k)$ in the lower half-plane, we have to analytically continue it there from the upper half-plane. (Using eq. (A2) directly in the lower half-plane would give another, unphysical sheet of $\gamma(\omega, k)$.)

Because $g(p_x)$ is even, $g'(p_x)$ is odd. From this, it follows that in the upper half-plane $\gamma(\omega, k)$ can have zeroes only on the imaginary axis. For $\omega = i\omega_i$ with $\omega_i > 0$, γ takes the form

$$\gamma(i\omega_i, k) = 1 + 4\pi G m^3 \int_{-\infty}^{\infty} dp_x \frac{p_x g'(p_x)}{k^2 p_x^2 + m^2 \omega_i^2} \tag{A4}$$

(in particular, it is purely real). The conditions on $g(p_x)$ guarantee that $p_x g'(p_x) < 0$ for any nonzero p_x. That means that the integral in (A4) is negative, so that at any fixed $k > 0$ $\gamma(i\omega_i, k)$ is a monotonically increasing function of ω_i. Consequently, at a given k it has at most one zero in the upper half-plane of ω. This zero, when it occurs, signals an instability

of the initial state with respect to fluctuations with that k. For example, such a zero always exists for $k \to 0$; its position, $\omega_i(0)$, is given by eq. (13).

Now let us see what happens as k increases. Zeroes of $\gamma(\omega, k)$, i.e. roots of eq. (A1), define a dispersion law $\omega(k)$. As long as, for a given k, the zero is still in the upper half-plane, we can continue to use eq. (A4). First, it follows from (A4) that $\omega_i(0)$ is an upper bound on $\omega_i(k)$. So, as we change k, a root cannot appear from infinity. Second, differentiating (A1) with respect to k and using again (A4), we find that, when $g(p_x)$ obeys the stated conditions, $d\omega_i(k)/dk$ is necessarily negative. So, as k increases, the root moves down towards the real axis. It reaches the real axis at the value $k = k_*$ determined by setting $\omega_i = 0$ in (A4):

$$k_*^2 = 4\pi G m^3 \left| \int_{-\infty}^{\infty} dp_x g'(p_x)/p_x \right| . \tag{A5}$$

(Note that there is no divergence at $p_x = 0$ here, because $g'(0) = 0$, see condition (iv).) We have already established that any root of (A1) in the upper half-plane is on the imaginary axis, and that such a root cannot appear from infinity. As a consequence, the point $\omega = 0$ is the only point where the root of (A1) can leave or enter the upper half-plane of ω. Because the corresponding value of k is unique, the root will not reappear in the upper half-plane at any $k > k_*$. We conclude that the collisionless instability is absent for all $k \geq k_*$.

A detailed picture of how the instability disappears can be obtained by expanding the original expression for γ, eq. (A2), in an asymptotic series about $\omega = 0$. The $i0$ prescription in (A2) will ensure that we are expanding on the correct sheet of $\gamma(\omega, k)$:

$$\gamma(\omega, k) = 1 + \frac{4\pi G m^3}{k^2} \int_{-\infty}^{\infty} dp_x \frac{g'(p_x)}{p_x - i0} \left(1 + \frac{m\omega/k}{p_x - i0} + O(\omega^2) \right) . \tag{A6}$$

For a smooth even $g(p_x)$, this evaluates to

$$\gamma(\omega, k) = 1 - \frac{k_*^2}{k^2} \left(1 + \frac{i\pi\omega m g''(0)/k}{\int_{-\infty}^{\infty} dp_x g'(p_x)/p_x} + O(\omega^2) \right) . \tag{A7}$$

Writing $k = k_* + \Delta k$ and expanding in small Δk, we find that the root of the dispersion equation has the form

$$\omega(\Delta k) = -i \frac{2\Delta k}{\pi m} \left| \frac{\int_{-\infty}^{\infty} dp_x g'(p_x)/p_x}{g''(0)} \right| + O((\Delta k)^2) . \tag{A8}$$

This expression shows explicitly that, as k increases past k_*, the root moves from the upper half-plane into the lower half-plane.

The structure of higher-order terms in (A7) is as follows: the coefficients of even powers of ω are all real, while the coefficients of odd powers are all imaginary. So, to any finite order in Δk, the root of the dispersion relation will remain purely imaginary even after it moves in the lower half-plane, and the mode corresponding to that Δk will be overdamped (non-oscillatory). This conclusion may be obviated by terms that are "nonperturbative" in Δk, i.e. are not seen in the asymptotic expansion (A6). We also stress that it applies only to fluctuations about a homogeneous state, not to a state that already contains clumps.

REFERENCES

[1] J. Jeans, Phil. Trans. **199A**, 1 (1902).

[2] P. J. E. Peebles, *The Large-Scale Structure of the Universe* (Princeton University Press, Princeton, 1980).

[3] N. N. Bogoliubov, J. Phys. USSR, **11**, 23 (1947).

[4] M. Yu. Khlopov, B. A. Malomed, and Y. B. Zeldovich, Mon. Not. R. Astron. Soc. **215**, 575 (1985).

[5] M. Bianchi, D. Grasso, and R. Ruffini, Astron. Astrophys. **231**, 301 (1990);

[6] Y. Nambu and M. Sasaki, Phys. Rev. D **42**, 3918 (1990).

[7] R. Ruffini and S. Bonazzola, Phys. Rev. **187**, 1767 (1969).

[8] D. Grasso, Phys. Rev. D **41**, 2998 (1990).

[9] S. Khlebnikov and I. Tkachev, hep-ph/9902272.

[10] L. P. Pitaevskiĭ, Uspekhi Fiz. Nauk, **168**, 641 (1998) [Physics-Uspekhi **41**, 569 (1998)].

[11] S. Khlebnikov, in: Strong and Electroweak Matter '97: Proceedings of the Conference, edited by F. Csikor and Z. Fodor (World Scientific, Singapore, 1998), p. 69.

[12] E. M. Lifshitz and L. P. Pitaevskiĭ, *Physical Kinetics* (Pergamon, Oxford, 1981).

[13] Yu. Kagan and B. V. Svistunov, Zh. Eksp. Teor. Fiz. **105**, 353 (1994) [JETP **78**, 187 (1994)]; K. Damle, S. N. Najumdar, and S. Sachdev, Phys. Rev. A **54**, 5037 (1996).

[14] M. Colpi, S. L. Shapiro, and I. Wasserman, Phys. Rev. Lett. **57**, 2485 (1986); I. I. Tkachev, Pis'ma Astron. Zh. **12**, 726 (1986) [Sov. Astron. Lett. **12**, 305 (1986)].

[15] E. Seidel and W.-M. Suen, Phys. Rev. Lett. **72**, 2516 (1994).

[16] I. I. Tkachev, Phys. Lett. B **261**, 289 (1991).

[17] E. W. Kolb and I. I. Tkachev, Phys. Rev. Lett. **71**, 3051 (1993).

FIGURES

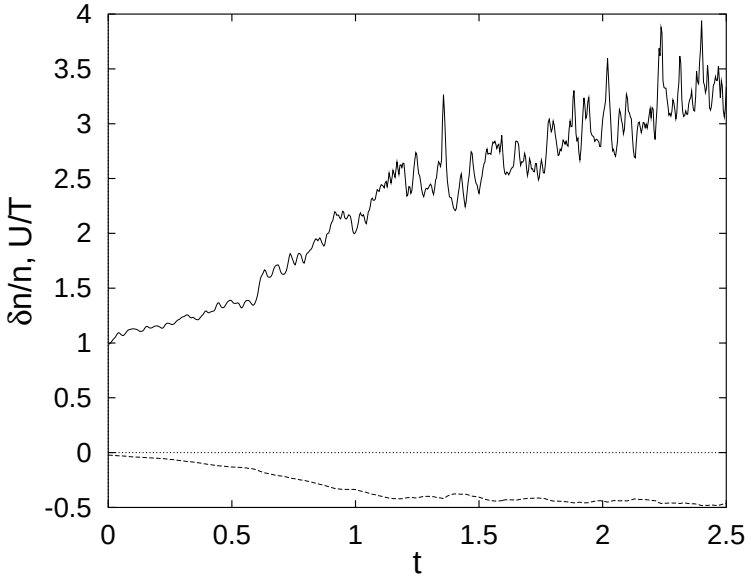

FIG. 1. Illustrates crossover from the collisionless instability to a scattering regime. These plots are for $B = 20$ and $L = 4.25$. Solid line shows the density contrast; dashed line—the ratio of the total potential and kinetic energies. The crossover occurs around $t = 1.2$.

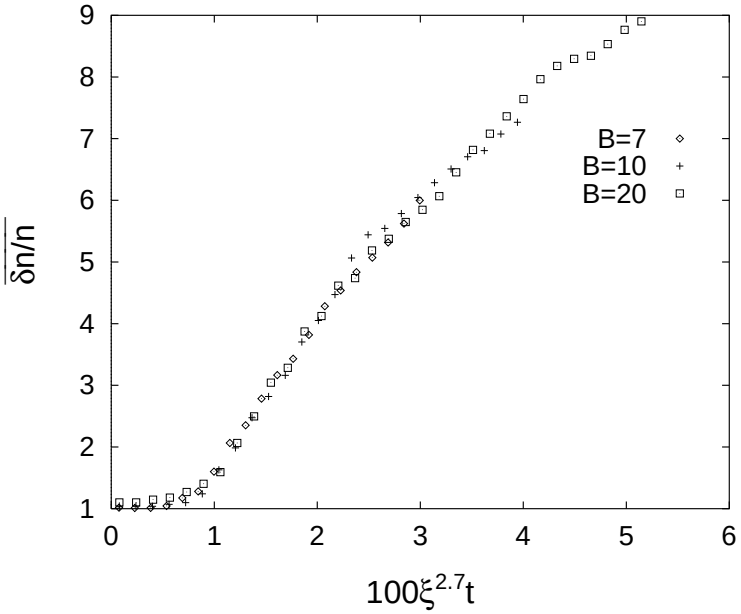

FIG. 2. Density contrast averaged over intervals of time, as a function of rescaled time. Each symbol is at the center of an interval over which the averaging is carried out. All data are for $L = 3.5$. The data for $B = 7$ and $B = 20$ correspond to the same realization of random initial phases; those for $B = 10$—to a different one.

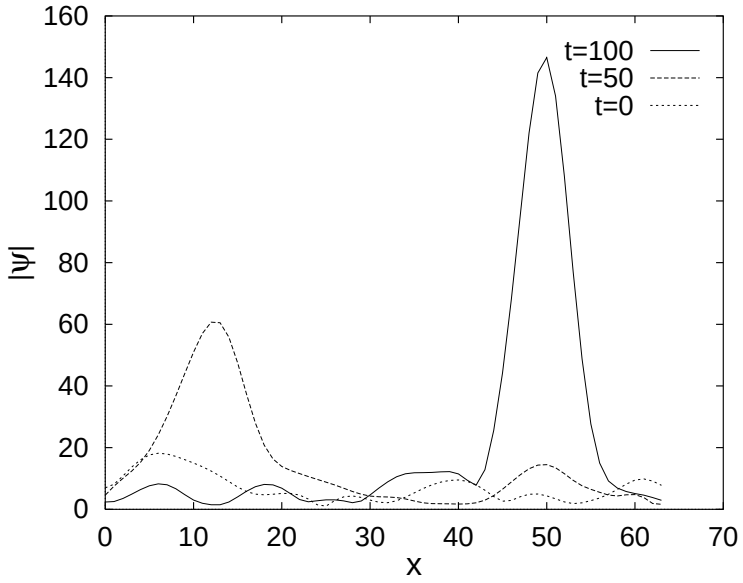

FIG. 3. Profile of $|\psi|$ along a line passing through the maximum of $|\psi|$, at different moment of time. Because the location of the maximum moves, the actual lines are different at different moments (although they are chosen parallel). These plots are for $L = 3.5$ and $B = 7$. The coordinate along the line is in units of the lattice spacing.

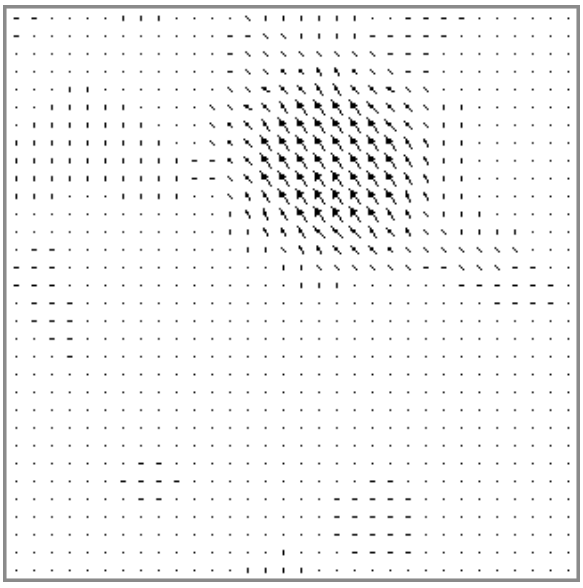

FIG. 4. Distribution of the field ψ on a quarter of a spatial slice at time $t = 100$, for $L = 3.5$ and $B = 7$. The slice cuts through the star's center. The length of an arrow corresponds to $|\psi|$ on a given site, and the angle the arrow makes clockwise from 12 noon—to the phase of ψ. Arrows on all sites with $|\psi| \geq 70$ have the same (maximal) length.